ISSN: 3069-1753

Research Article

Global Journal of Agriculture, Earth & Environmental Science

OPENPUB GLOBAL PUBLISHERS

Received: 12-08-2025 Accepted: 16-08-2025 Published: 27-08-2025

Volume 1 | Issue 2

Exploring The Mechanism of Fruit Expansion in Strawberry Mutants Through A Joint Study of Anatomical Structures, Phytohormones and The Transcriptome

Yilin Yang[1+], Zihang Ouyang[1+], Siqi Dai[1], Yuanxiu Lin[1], Yunting Zhang[1], Mengyao Li[1], Qin Chen[1], Yong Zhang[1], Haoru Tang[1], Ya Luo[*1]

[1]College of Horticulture, Sichuan Agricultural University, Chengdu 611130, China.

[*]**Corresponding author:** Luo., Ya, College of Horticulture, Sichuan Agricultural University, Chengdu 611130, China.

Citation: Luo., Y, Yang., Y, Ouyang., Z, Dai., S, Lin., Y, et al. (2025). Exploring The Mechanism of Fruit Expansion in Strawberry Mutants Through A Joint Study of Anatomical Structures, Phytohormones and The Transcriptome. Glob. J. Agric. Earth Environ. Sci. 1(2), 1-18.

Abstract

Fruit size in cultivated strawberry (Fragaria × ananassa Duch.) is a key trait affecting farmers' profitability. This study identified a mutant (MT) from 'Benihoppe' strawberry (WT) with larger and heavier mature fruits. To analyze the molecular mechanism of fruit expansion and quality associations, we performed a combined analysis integrating physiological indicators and the transcriptome. The results showed that MT fruits were primarily driven by cortical cell expansion from the large green (LG) to partial red (PR) stages, with continued pith and cortical cell division contributing to the large-fruit phenotype during PR to fully red (FR) stages. This expansion concomitantly altered flavor quality, with mature MT fruits displaying elevated fructose, glucose and cyanidin content but reduced pelargonidin-3-glucoside (Pg3G) compared to WT. Notably, endogenous indole-3-acetic acid (IAA) level was consistently elevated in MT throughout development, whereas abscisic acid (ABA) level was significantly suppressed during the LG and FR stages. A strong negative correlation between these phytohormones was observed. Transcriptomic profiling further indicated attenuated signaling capacity for both IAA and ABA pathways specifically during the LG and PR stages. Using weighted gene co-expression network analysis (WGCNA), the key gene regulating strawberry fruit size was identified as FaIAA29. Further assays confirmed that FaIAA29 localized to the nucleus and negatively regulated fruit cell size, anthocyanin accumulation, and coloration while promoting cell density. Yeast one-hybrid and dual-luciferase assays validated FaIAA29 binding to the FaMIT promoter and its strong repression of FaGluRS promoter activity. These findings help to elucidate the molecular functions of FaIAA29 in fruit growth.

Keywords: Strawberry, Fruit size, Quality, Phytohormone, Aux/IAA

Introduction

As organs unique to angiosperms, fruits provide humans with essential vitamins, dietary fiber and carbohydrates [1]. Fruit morphological development hinges on the dynamic balance between cell number and size. Cell division frequency and cycle duration govern cell number, while cellular expansion governs cell size[2,3]. Research in model plants has demonstrated that fruit weight 2.2 *(FW2.2)* negatively regulates tomato fruit size by inhibiting early cell division [4], whereas *SlFW3.2* promotes fruit enlargement by enhancing cell division [5]. Expansins (EXPs) mediate cell wall relaxation to promote cell expansion [6]. Overexpression of *NtEXPA1* enlarges individual cells, resulting in larger tobacco leaves and thicker stems [7], and *OsEXPA4* positively regulates cell size to promote larger rice grains [8], collectively confirming the role of *EXPs* in facilitating fruit enlargement through cell wall expansion. However, the regulatory mechanisms underlying fruit size in perennial fruit trees remain comparatively unexplored.

The cultivated strawberry (*Fragaria* × *ananassa* Duch.) serves as an ideal model system for studying non-climacteric fruit development and ripening. During early strawberry fruit development, auxin, gibberellin acid (GA) and cytokinin (CTK) influence fruit set and development by regulating cell division and expansion. Meanwhile, abscisic acid (ABA) dominates the ripening process [9]. The signaling pathway is an important part of auxin research. Under conditions of low auxin concentration, aux/indole-3-acetic acid (Aux/IAA) repressor proteins form heterodimers with auxin response factors (ARFs). This inhibits the transcription of downstream genes by preventing ARFs from binding to their promoters. Under conditions of high auxin concentration, the transport inhibition response 1 (TIR1)/auxin signaling F-box (AFB) receptor protein binds to structural domain II of Aux/IAA. By mediating ubiquitination to degrade the latter, the released ARF binds to the promoter of small auxin up-regulated RNAs (SAURs) and regulates transcription of downstream genes [10,11]. Studies show that silencing *SlIAA17* elevates endoreduplication levels in tomato pericarp cells, increases cell size and promotes larger fruit [12]. Overexpression of *MdAux/IAA2* inhibits apple fruit weight and cell size [13]. Additionally, knockout of either *SlARF8A* or *SlARF8B* produces a small-fruit phenotype in tomato, with the double mutant fruits being even smaller [14]. These findings collectively implicate Aux/IAA-ARF modules in fruit size regulation across horticultural crops.

In strawberry fruit, ABA governs ripening through the core signaling cascade which comprises pyrabactin resistance (PYR)/PYR1-like (PYL)/regulatory component of ABA receptor (RCAR), protein phosphatase 2C (PP2C) and SNF1-related protein kinase 2 (SnRK2) [15]. During the initial stage of woodland strawberry fruit development, auxin and GA promote the expression of the ABA catabolism gene *cytochrome P450 monooxygenase* (*CYP707A4*), thereby reducing ABA levels to promote strawberry fruit enlargement. Exogenous application of ABA in the early stages of strawberry fruit development also significantly inhibits fruit enlargement [16]. However, exogenous application of 1-naphthylacetic acid (NAA) can delay strawberry fruit coloring [17]. Additionally, *SlPP2CC2*-mediated ABA signaling can co-regulate tomato fruit development with *SlSAUR*-mediated auxin signaling [18]. While the above studies have revealed the antagonism between IAA and ABA, the mechanism by which they synergistically regulate strawberry fruit development remains unclear.

Development of pith and cortex tissues critically determines strawberry fruit morphology and size [19]. However, consistent harvesting of strawberry fruits exceeding 25 g throughout the production season remains an unresolved industry challenge. The 'Benihoppe' strawberry dominates the Chinese market due to its uniform shape, high yield and superior quality. This study identified a stably inherited large-fruit mutant (MT) in field conditions, exhibiting significantly greater fruit weight, transverse diameter and longitudinal diameter than normal 'Benihoppe' (WT). Integrated approaches including high-performance liquid chromatography (HPLC), paraffin sectioning, HPLC-tandem mass spectrometry (HPLC-MS/MS), and transcriptomics were employed to investigate physiological and molecular mechanisms underlying fruit size divergence during development and ripening. Our results demonstrate that significant fruit size and weight differentiation between MT and WT primarily occurs from large green (LG) to partial red (PR) stages, dominantly driven by cortical cell expansion. Continued cell division in pith and cortex during PR to fully red (FR) stages further contributes to the large-fruit phenotype. This expansion correlates with altered accumulations of soluble sugars and anthocyanins. Furthermore, these differences are closely associated with variations in endogenous indole-3-acetic acid (IAA) and abscisic acid (ABA) levels, as well as differential signaling capacities of IAA and ABA in WT versus MT. Functional validation identified *FaIAA29* as a key transcriptional repressor of strawberry fruit cell size. This study demonstrates for the first time the application potential of *Aux/IAA* genes within the auxin signaling pathway for regulating strawberry fruit cell size, establishing cellular dimensions as a breeding target for fruit size enhancement.

1. Materials and Methods

1.1 Plant Material

Cultivated strawberry (*Fragaria* × *ananassa* Duch.) 'Benihoppe' and its mutant plants were planted at the strawberry picking base in Jinggang Village, Pidu District, Chengdu City, Sichuan Province, China. The mutant was grown from September to December 2022 in 'Benihoppe' strawberry was found during cultivation. Organs at different developmental stages (roots, stems, leaves and flowers) were collected regularly, and fruit developmental stages were classified as small green (SG), large green (LG), white (W), partially red (PR) and fully red (FR) depending on the color of the receptacle. All samples were stored at -80°C for subsequent

experiments. There were three biological replicates for each developmental stage and six strawberry fruits per replicate. Tobacco (*Nicotiana benthamiana*) was incubated in an artificial climate chamber at 25°C with 16 hours of light / 8 hours of darkness and 70% relative humidity.

1.2 Morphophysiological characterization

Fruit weight was determined using an electronic scale. Fruit shape index was expressed as the transverse diameter of the fruit divided by the longitudinal diameter. *L**, *a** and *b** values of the fruit were determined using a colorimeter (CR-400, Konica Minolta). Fruit hardness was determined using a hardness tester (FR-5105, LUTRON).

1.3 Determination of strawberry fruit quality

The contents of major organic acids (citric acid, malic acid and oxalic acid), ascorbic acid, anthocyanins (Pg3G and cyanidin) and sugars (fructose, sucrose and glucose) in the fruits were detected by a modified HPLC, and all of them were set up in three independent biological replicates.

For the determination of sugars, 0.3 g of the sample was extracted with 2 mL of ultrapure water in a water bath at 80℃ for 15 min, centrifuged and filtered with a 0.45 μM filter, and then separated on an Athena NH2-RP column with isocratic elution of acetonitrile:water (80:20) as the mobile phase (1 mL/min, 25℃) for 10 min, and then detected by an oscillometric refractive detector with a 10 μL injection volume.

For the determination of organic acids, 0.3 g of sample was extracted with 4 mL of 0.2% phosphoric acid solution, centrifuged and filtered, and then separated on a Polaris C18-A column with the mobile phase consisting of 3% methanol + 97% 0.2% phosphoric acid (0.8 mL/min), detected by UV 210 nm, isocratic elution for 10 min, and the injection volume was 20 μL.

For the determination of anthocyanins, 0.3 g of the sample was extracted with 1% HCl-methanol (24 hours at 4℃ protected from light), and the combined extracts were filtered and separated on a Poroshell 120 SB-C18 column (Agilent) with UV 210 nm detection, and the mobile phases were gradient eluted from A (5% formic acid) and B (methanol) at a flow rate of 1 mL/min with an injection volume of 10 μL. All assays were performed using an Agilent 1260 Infinity II HPLC system.

1.4 Section preparation and cellular observation

Strawberry fruits were fixed in FAA fixative (38% formaldehyde: glacial acetic acid: 75% alcohol=1:1:18) for 1-2 days, then dehydrated with gradient ethanol, and the material was made transparent with xylene and ethanol. After transparency, the material was immersed in wax, embedded in paraffin, then sectioned and dried. Sequentially, the material was deparaffinized with xylene, treated with gradient ethanol, stained with 1% aqueous solution of safranin for 3 hours, restained with 0.5% fast green ethanol solution for 30 seconds, and finally treated with xylene and sealed with neutral gum. The sections were observed with an OLYMPUS SZX7 stereomicroscope at 3.2× and 5.6× magnification, and the cell size was determined with Image J-win64 software. The area of strawberry fruits and cells was calculated by using horizontal and vertical calculations, and the area of 40 cells was determined by selecting them from five parts of the sections: upper, lower, left, right, and center, and the formula for calculating the number of cells was as follows: $N=S^{fruit}/S^{cell}$.

1.5 Determination of endogenous hormone content

The contents of endogenous plant hormones (ABA, IAA, SA and GA_3) were quantified in whole strawberry fruit tissue (receptacle and achene) using HPLC-MS/MS. After grinding with liquid nitrogen, 0.2 g of the sample was added into the internal standard, extracted with acetonitrile solution at 4℃ overnight, centrifuged and the supernatant was extracted twice and combined with the

supernatant, cleaned up by C18 and GCB, concentrated by nitrogen blowing, redissolved with 400 μL methanol and passed through 0.22 μM organic phase filtration membrane, and then stored at – 20°C for examination. Chromatographic separation was performed on a Poroshell 120 SB-C18 column (2.1×150 mm, 2.7 μM) with a gradient elution of methanol-water solution containing 0.1% formic acid (20%-80% methanol, 0-10.5 min) at a flow rate of 0.3 mL/min and a column temperature of 30°C, with an injection volume of 2 μL. A linear standard curve was used in the range of 0.1-200 ng/mL. A linear standard curve of 0.1-200 ng/mL (with 20 ng/mL internal standard) was used for quantitative analysis.

1.6 Transcriptome sequencing and analysis

Total RNA was extracted from WT and MT fruits at three developmental stages (LG, PR and FR) using an improved CTAB method [20]. Eighteen libraries (3 biological replicates per stage) were constructed and sequenced by Chengdu JiYu Biotechnology Co., Ltd. The RNA library was then sequenced on the Illumina Hiseq platform. Raw reads were quality filtered (Q < 20) and splice sequences removed using Trim Galore (v0.6.6). Clean reads were compared to the cultivated strawberry (*Fragaria* × *ananassa*) 'Benihoppe' reference genome (v1.0) downloaded on GDR (https://www.rosaceae.org/) by HISAT2 (v2.2.1). fragments per kilobase of script per million fragments mapped (FPKM) was used as an indicator to measure gene expression levels, with the threshold for significant differential expression being an absolute $|\log_2 \text{Fold Change}| \geq 2$ and False Discovery Rate < 0.05. KEGG categories were used to annotate DEGs.

The transcriptome data were analyzed by WGCNA to obtain the gene co-expression similarity matrix, which was grouped based on the TOM method using hierarchical clustering. Based on the phenotypic data of fruit developmental stages, the association analysis was performed with modules, and the most significant modules were selected for analysis. Interaction networks were created using Cytoscape (v.3.10.2) software.

1.7 Identification and validation of gene family members

Blast comparisons (e-value < e^{-10}) were performed in TBtools software (v. 2.225) using protein sequences of target genes from *Arabidopsis* downloaded from the TAIR (https://www.arabidopsis.org/), and pre-screened family members were subsequently submitted for validation to the NCBI conserved structure domain database (https://www.ncbi.nlm.nih.gov/Structure/cdd/wrpsb.cgi) for validation. The phylogenetic tree of IAA29 was constructed in MEGA 7 (7.0.26) software using the Neighbor-Joining (NJ) method.

1.8 Real-time quantitative PCR (RT-qPCR)

RT-qPCR was used to detect gene expression. A 20 μL reaction system was set up according to the instructions of SYBR Green I (Thermo Fisher). All RT-qPCR reactions were repeated three times. Quantitative primers are shown in Table S1.

1.9 Subcellular localization analysis

The full-length coding region of the *FaIAA29* was amplified and ligated into a green fluorescent protein (GFP) fusion expression vector driven by the CaMV 35S promoter (Table S1). To investigate the subcellular localization of *FaIAA29*, 35S:*FaIAA29*-GFP was cotransformed into tobacco leaves with a nuclear localization marker construct (NLS-RFP) fused with red fluorescent protein (RFP). After 3 days of incubation in the dark, tobacco leaves were harvested and visualized using a confocal laser scanning microscope (FV3000; OLYMPUS).

1.10 Transient overexpression of FaIAA29 in strawberry fruit

Fruits of uniform maturity and size and normal fruit type were collected for injection. A pair of specific primers was designed for amplification of the complete CDS sequence of *FaIAA29*, followed by insertion of the target fragments into the pCAMBIA 1301

vector (Table S1), respectively. *Agrobacterium tumefaciens* GV3101-mediated genetic transformation method was used to introduce the pCAMBIA 1301 recombinant vector carrying *FaIAA29* into white stage strawberry fruits, and the empty vector transformant was used as the control, and the overexpression bacterial solution and the empty control were injected into the two sides of the fruits respectively, and then after one day of injection, the same method was used to replenish the injection at the same part, and the maceration was carried out for a total of 7 days. After that, the phenotypes were observed, then the achenes of the fruit cortex were retained, the pith portion was discarded, and the fruits were ground with liquid nitrogen and stored in a refrigerator at -80°C for later use. The experiment was set up with three biological replicates and eight fruits in each replicate.

The transiently overexpressed strawberry fruit parts were subjected to paraffin sectioning according to the same method of 4.4, and the experiment was set up with 3 biological replicates and 2 technical replicates. The small cells in the middle of the section were ignored when observing the cell morphology and counting.

1.11 Cis-regulatory element analysis

Sequences within 2000 bp upstream of the *FaGluRS* and *FaMIT* start codons were extracted, respectively, and cis-elements were predicted using PlantCARE (https://bioinformatics.psb.ugent.be/webtools/plantcare/html/) and visualized using TBtools for visualization.

Potential binding sites of *FaIAA29* to the *FaGluRS* and *FaMIT* promoters were screened using the TFDB (https://planttfdb.gao-lab.org/).

1.12 Yeast one-hybrid (Y1H) assay

A bait reporter vector was constructed by inserting promoter fragments with *FaGluRS* (P1-P2) and *FaMIT* (P1-P3) into the pAbAi vector. The CDS sequence of *FaIAA29* was inserted into pGADT7 vector to form pGADT7-*FaIAA29* fusion vector (Table S1). The bait reporter vector was transformed into Y1H yeast using a transformation system. The pGADT7- *FaIAA29* vector was transformed into positive bait reporter yeast, which was subsequently grown on SD/-Leu-and SD/-Leu/AbA mediums. For verification, dilutions of 1, 10, 100 and 1000 times were utilized.

1.13 Dual-luciferase assay

A transient dual-luciferase assay was used to assess the trans-activation activity of the *FaIAA29* on the *FaGluRS* and *FaMIT* promoters. The coding regions of the transcription factors were cloned into the pCAMBIA 1301 vector under the control of the CaMV35S promoter as an effector, and 1500 and 2000-bp fragments of the *FaGluRS* and *FaMIT* promoters, respectively, were introduced into the pGreenII 0800-LUC vector as reporters (Table S1). The constructed effector and reporter plasmids were introduced into *Agrobacterium rhizogenes* (GV3101) to cotransform tobacco. The dual-luciferase assay kit (Yeasen) was used to determine the luciferase activities of LUC and REN, and the results were based on the relative ratio of LUC to REN.

1.14 Statistical analysis

Data were analyzed using Excel 2019 and SPSS 24.0, with Tukey's test ($P < 0.05$) for significance and Pearson's correlation for associations. Bioinformatics analysis and graphing were performed using GraphPad Prism 8 and The CNSknowall platform (https://cnsknowall.com), and the data were expressed as mean ± standard deviation (SD), and the values of different letters above the bars were significantly different from each other. values are significantly different (P <0.05), and * and ** represent significant and highly significant differences, respectively.

2. Results

2.1 Morphological and physiological characteristics of 'Benihoppe' and its mutant fruit during development

Significant morphological differences in floral organs and developing fruits were observed between normal 'Benihoppe' (WT) and its large-fruit mutant (MT) (Fig. 1A). Throughout fruit development, both transverse diameter, longitudinal diameter and fresh weight increased continuously in both materials. After the PR stage, the transverse diameter and fruit weight of MT were significantly higher than WT (Fig. 1B, C, D). From LG to PR stage, MT fruits exhibited a substantial 107.0% increase in fresh weight. In contrast, WT fruits showed a significantly lower increase of only 36.6%. From PR to FR stage, MT maintained a considerably high growth rate (62.1%), while WT growth during this period measured 55.3%. Similarly, regarding fruit dimensions during the LG-PR transition, MT displayed significantly higher growth rates for transverse diameter (31.6%) and longitudinal diameter (23.7%) than WT fruits (11.9% and 4.6%, respectively). During the subsequent PR-FR period, the transverse diameter growth rate in MT (20.4%) was comparable to that in WT (19.8%). However, MT fruits still exhibited a significantly greater longitudinal diameter growth rate (10.9%) during this phase than WT fruits (4.9%). Consequently, MT fruits demonstrated significantly larger transverse and longitudinal dimensions than WT at the FR stage (Fig. 1C, D). However, further comparison revealed no significant difference in the fruit shape index (transverse diameter / longitudinal diameter) between mature MT and WT fruits (Fig. 1E). These results demonstrate that the significant increase in fruit weight and size for MT predominantly occurred during the LG to PR stage. Conversely, the primary phase of growth for WT extended from PR to FR. Furthermore, the LG to PR period as the critical developmental window responsible for establishing the significant difference in fruit size and weight between the two materials.

For fruit coloration, L^* values progressively decreased, while a^* values progressively increased during development in both materials. Importantly, mature WT and MT fruits showed no significant difference in either L^* or a^* values (Fig. 1F, G). Furthermore, fruit firmness gradually decreased as development progressed in both materials, with no significant difference in firmness detected between MT and WT at the FR stage (Fig. 1H). These results suggest that the increased size and weight in MT fruits does not affect final color or hardness.

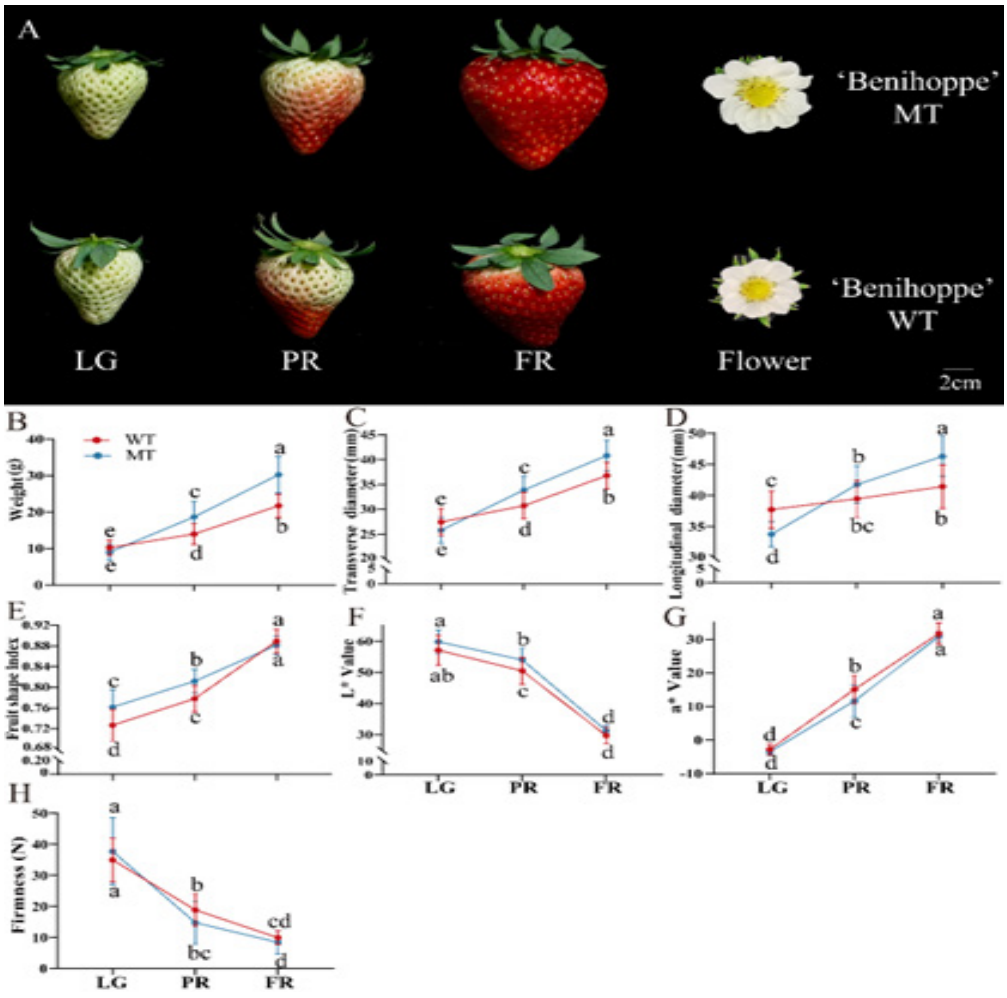

OPENPUB Global Publishers

Figure 1. Morphological and physiological characteristics during strawberry fruits development. Normal 'Benihoppe' and mutant strawberry: morphology (A), weight (B), transverse diameter (C), longitudinal diameter (D), fruit shape index (E), *L** value (F), *a** value (G) and firmness (H). Differences in lowercase letters (a, b, c) indicate significant differences and identical letters indicate no significant differences.

2.2 Analysis of fruit quality components during fruit development in 'Benihoppe' and its mutant

During fruit development, sucrose, fructose and glucose levels increased in both WT and MT. MT exhibited significantly lower sucrose concentrations than WT at LG, PR and FR stages (Fig. 2A). In contrast, MT accumulated higher fructose and glucose levels than WT after the PR stage (Fig. 2B, C). Further analysis of the sugar component ratios revealed that the sucrose proportion in WT increased from 42.1% in the LG stage to 47.4% in the FR stage, while that in MT increased from 19.3% to 24.2% during the same period. Additionally, the glucose and fructose proportions in MT decreased from 80.7% to 75.8%, However, it remained significantly higher than that of WT, which decreased from 57.9% to 52.6% (Figure 2J). These results suggest that the sugar accumulation in MT fruits features low sucrose and high monosaccharide content.

Citric acid constituted the predominant organic acid in both materials. MT accumulated significantly higher citric acid than WT throughout development (Fig. 2D). Malic acid level in MT decreased sharply after the PR stage (Fig. 2E). Oxalic acid, the least abundant acid, declined progressively during ripening and was consistently lower in MT than WT (Fig. 2F). Ascorbic acid increased gradually in both materials without significant differences at PR and FR stages (Fig. 2G). Compositional analysis showed the citric acid proportion in MT increased from 68.7% at LG to 82.2% at FR, whereas that in WT remained stable (61.7% to 61.4%). Concurrently, the malic acid proportion decreased from 24.7% to 10.6% in MT but only from 38.2% to 36.2% in WT (Fig. 2K). Collectively, MT fruits feature citric acid-dominant acid accumulation.

Pg3G was undetectable in WT at LG stage but present at trace levels in MT. At the PR stage, MT fruits contained more Pg3G than WT, while at FR stage, WT showed higher Pg3G accumulation than MT (Fig. 2H). Cyanidin were detected only in ripe fruits: MT accumulated 8.88 μg/g (PR) and 22.07 μg/g (FR), while WT accumulated 12.78 μg/g solely at FR stage (Fig. 2I). Thus, ripe MT fruits accumulate less Pg3G but more cyanidin than WT.

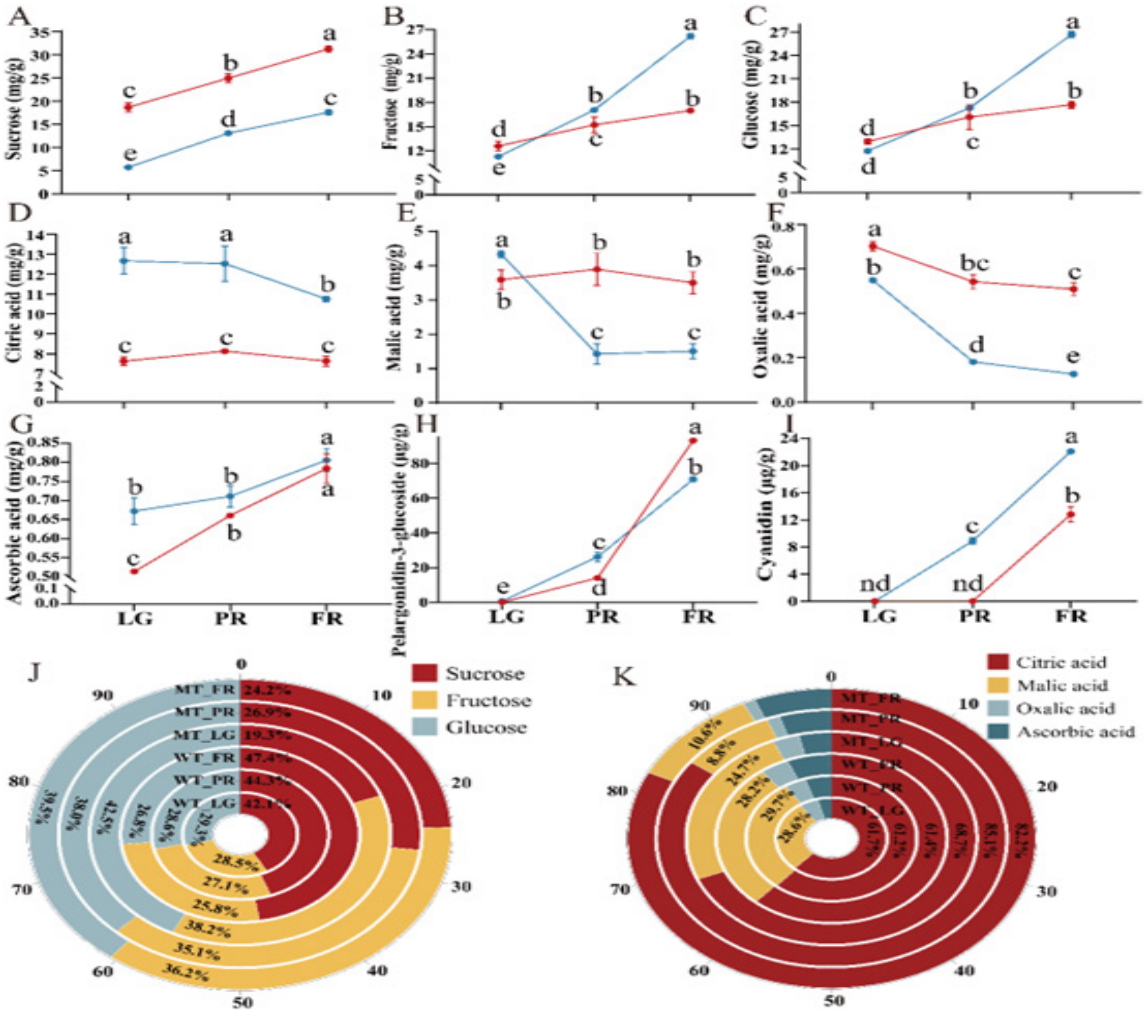

OPENPUB Global Publishers

Figure 2. Dynamic changes of sugars, organic acids and anthocyanins in strawberry fruit development. The contents of sucrose (A), fructose (B), glucose (C), citric acid (D), malic acid (E), oxalic acid (F), ascorbic acid (G), Pg3G (H) and cyanidin (I). Ratio of sugar components (J), ratio of organic acid and ascorbic acid components (K) in LG, PR, FR stage of WT and MT strawberry fruits. ND: not detected.

2.3 Changes in cell morphology and number during fruit development of 'Benihoppe' and its mutants

To investigate developmental differences at the cellular level, we analyzed paraffin sections of WT and MT fruits across three developmental stages (LG, PR and FR). Based on strawberry fruit anatomy, the longitudinal section was divided into the pith and cortex (Fig. 3A). In the pith, WT exhibited significantly enlarged cells from LG to PR stage, followed by reduced size at FR stage (Fig. 3B, D). Pith cell size in MT remained stable throughout development. Pith cell number showed no significant change in WT across stages, whereas MT displayed increased cell numbers from PR to FR stage (Fig. 3E). Linear correlation analysis indicated non-significant relationships between weight and both pith cell number/size (Fig. 3F).

Cortical cells expanded progressively in both materials. WT cortical area increased continuously: 9,312 μm² (LG) to 28,974 μm² (FR). MT cortical cells reached near-maximal size earlier: 13,845 μm² (LG) to 28,749 μm² (PR) (Fig. 3C, D). Cortical cell number in WT decreased significantly during LG to PR before stabilizing. In MT, it decreased during LG to PR then increased at FR (Fig. 3E). Importantly, a significant positive correlation existed between cortical cell size and weight (Fig. 3G), establishing cortical expansion as the primary determinant of fruit size differences. Persistent cell division in pith and cortex during PR-FR stages also contributed to MT enlargement.

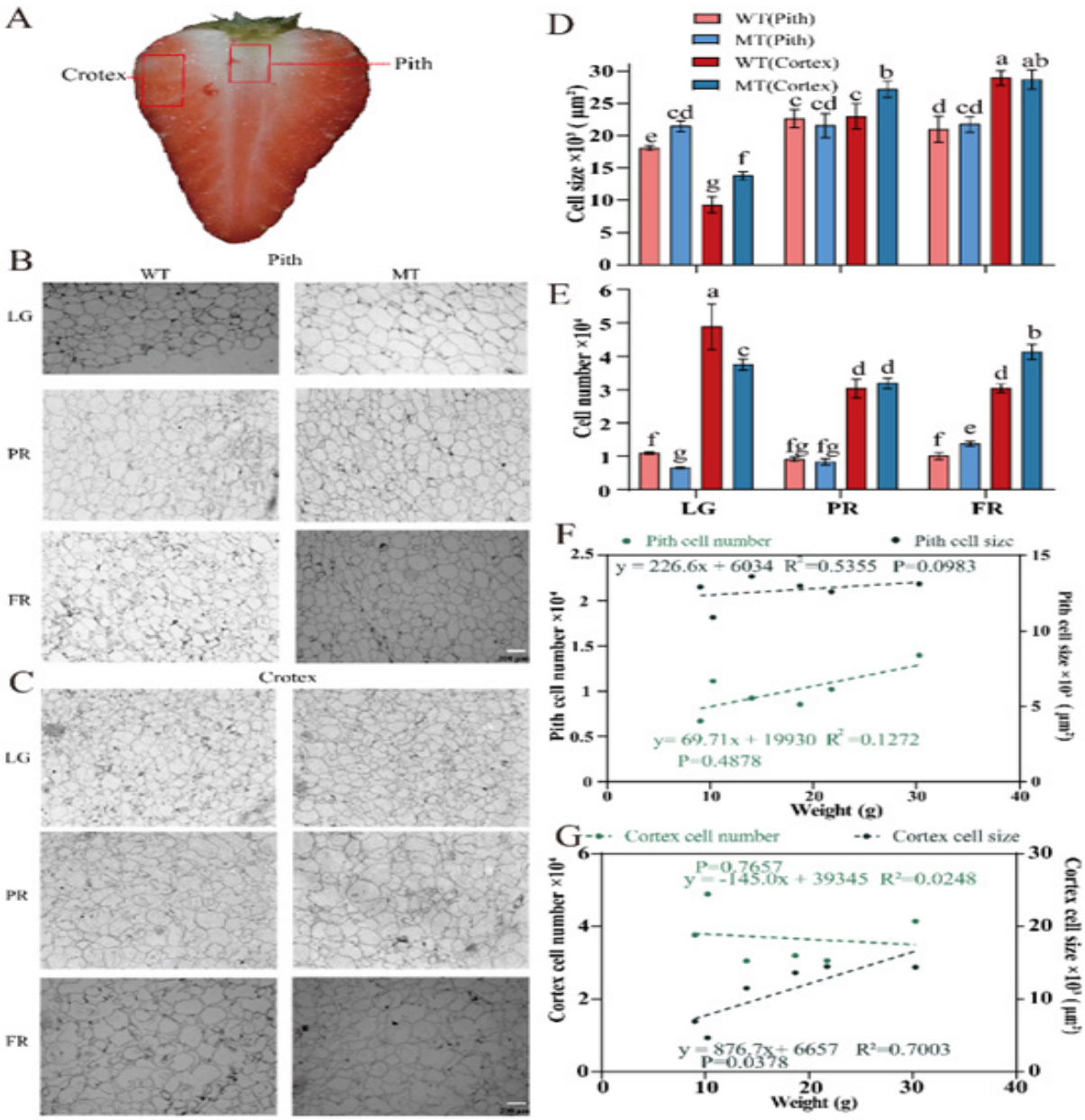

Figure 3. Dynamic changes in cell morphology and number during strawberry fruit development. Longitudinal section of the fruit (A), microscopic images of cells in the pith (B) and cortex (C) regions at different developmental stages of the fruit, changes in individual cell size (D) and total cell number (E) at different developmental stages of the fruit. Correlation analyses between cell traits (number and size) and weight for pith (F) and cortex (G). ($^{*}P < 0.05$, $^{**}P < 0.01$).

2.4 Differences in endogenous phytohormones in 'Benihoppe' and its mutant fruit

Endogenous levels of IAA, GA_4, ABA and SA were quantified in WT and MT fruits across developmental stages. IAA levels declined progressively in both materials, with MT exhibiting consistently higher level than WT at all stages (Fig. 4A). GA_4 showed similar temporal patterns in WT and MT, though lower GA_4 level was detected in MT specifically at LG stage (Fig. 4B). ABA accumulated during ripening, while MT displayed reduced ABA at LG and FR stages and elevated ABA at PR stage compared to WT (Fig. 4C). SA level was persistently lower in MT throughout development (Fig. 4D).

In this study, correlation analysis was used to examine how fruit size and quality characteristics are related. The study found that fruit weight positively correlated with transverse diameter, fruit shape index, fructose, glucose, Pg3G, cyanidin content and cortex cell size; and negatively correlated with IAA level. The transverse diameter was significantly positively correlated with longitudinal diameter, fruit shape index, fructose, glucose, Pg3G, cyanidin content and cortex cell size; and negatively correlated with IAA and GA_4 levels. The longitudinal diameter showed no significant correlation with any of the quality characteristics examined. Notably, IAA level was positively correlated with GA_4 level and negatively correlated with ABA level (Figure 4E). Since GA_4 primarily influences the longitudinal elongation of strawberry fruit [16], the lack of significant correlation between the longitudinal diameter and GA_4 level in this study is noteworthy. Therefore, differences in IAA and ABA levels may be the primary hormonal factors causing the size differences between WT and MT fruits, and fruit enlargement is closely related to the accumulation of monosaccharides and anthocyanins during development.

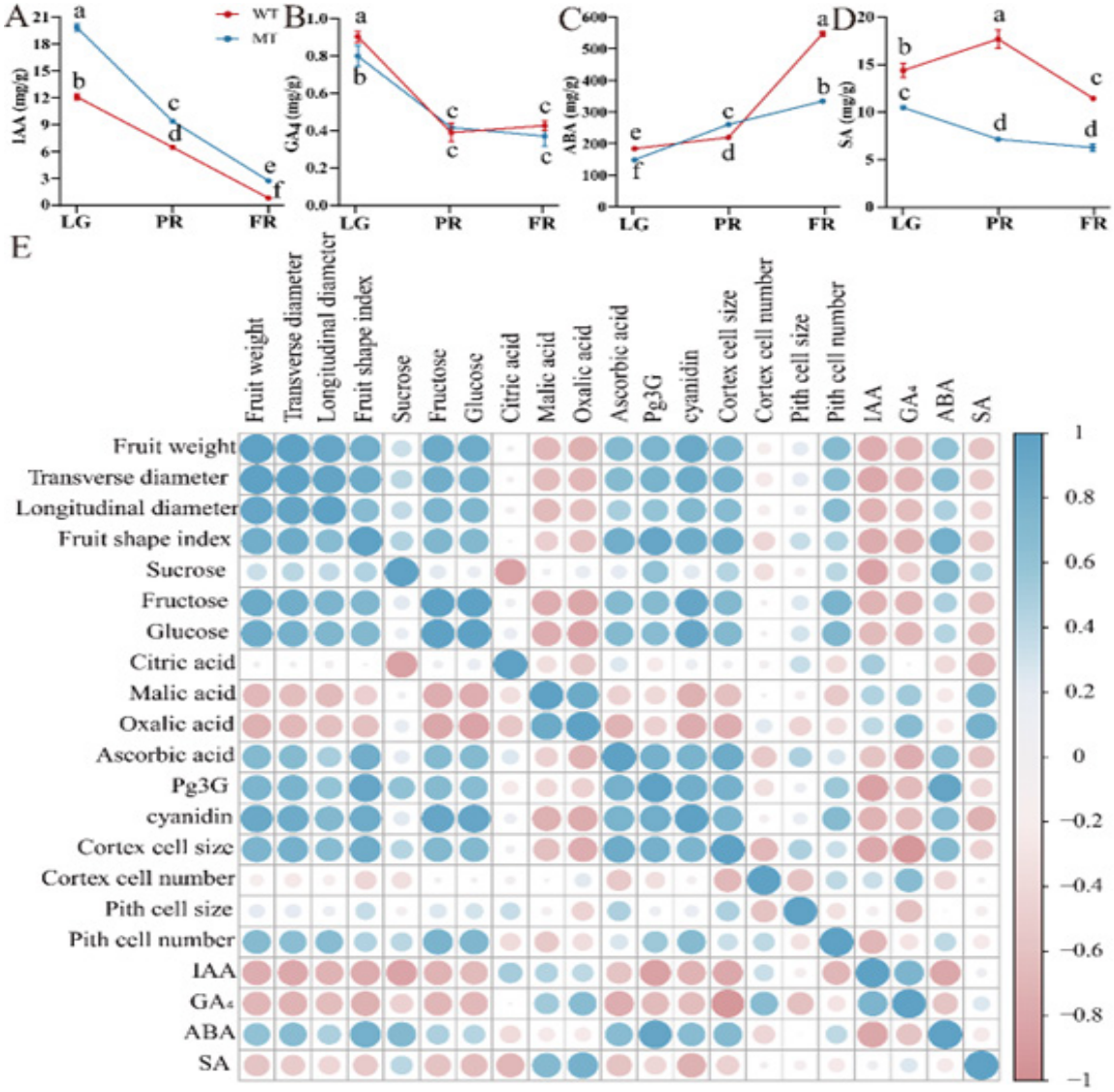

Figure 4. Content of endogenous phytohormones during strawberry fruit development. IAA (A), GA_4 (B), ABA (C) and SA content (D). Correlation analysis of physiological data (E).

2.5 Transcriptome analysis of strawberry fruit combined with WGCNA analysis

Transcriptome sequencing generated 18 high-quality RNA-seq datasets from WT and MT materials across three developmental stages (Table S2). Principal component analysis (PCA) indicated transcriptomic divergence between materials was greatest at FR stage (Fig. 5A). Differentially expressed genes (DEGs) between WT and MT were identified: 3,525 at LG, 1,526 at PR and 5,758 at FR stage (Fig. 5B and Table S3). KEGG enrichment analysis showed DEGs commonly enriched in phenylpropanoid biosynthesis, alpha-linolenic acid metabolism, biosynthesis of plant secondary metabolites and cutin, suberine and wax biosynthesis (Fig. S1B, C, D and Table S4).

To identify candidate genes associated with strawberry fruit size regulation, a gene co-expression network was constructed using WGCNA, identifying 16 distinct gene modules. We selected the MEblue module, which is significantly correlated with fruit shape index, cortex cell size, IAA and ABA, with correlation coefficients of 0.79, 0.70, -0.71 and 0.99, respectively (Fig. 5C and Fig. S1A). Intersection analysis between MEblue module genes and stage-specific DEGs yielded 31 overlapping candidates (Fig. 5D). Cluster heatmap analysis revealed that distinct dynamics for Fxa2Bg02917: its transcript levels increased progressively during MT development, consistent with the growth trends of fruit size and weight, while displaying rise-then-decline patterns in WT (Fig. 5E). Based on combined fold-change ($|\log_2 FC| \geq 3$) and homologous gene annotations from NCBI (Table S3), Fxa2Bg02917 was identified as a key candidate gene that regulates strawberry fruit size.

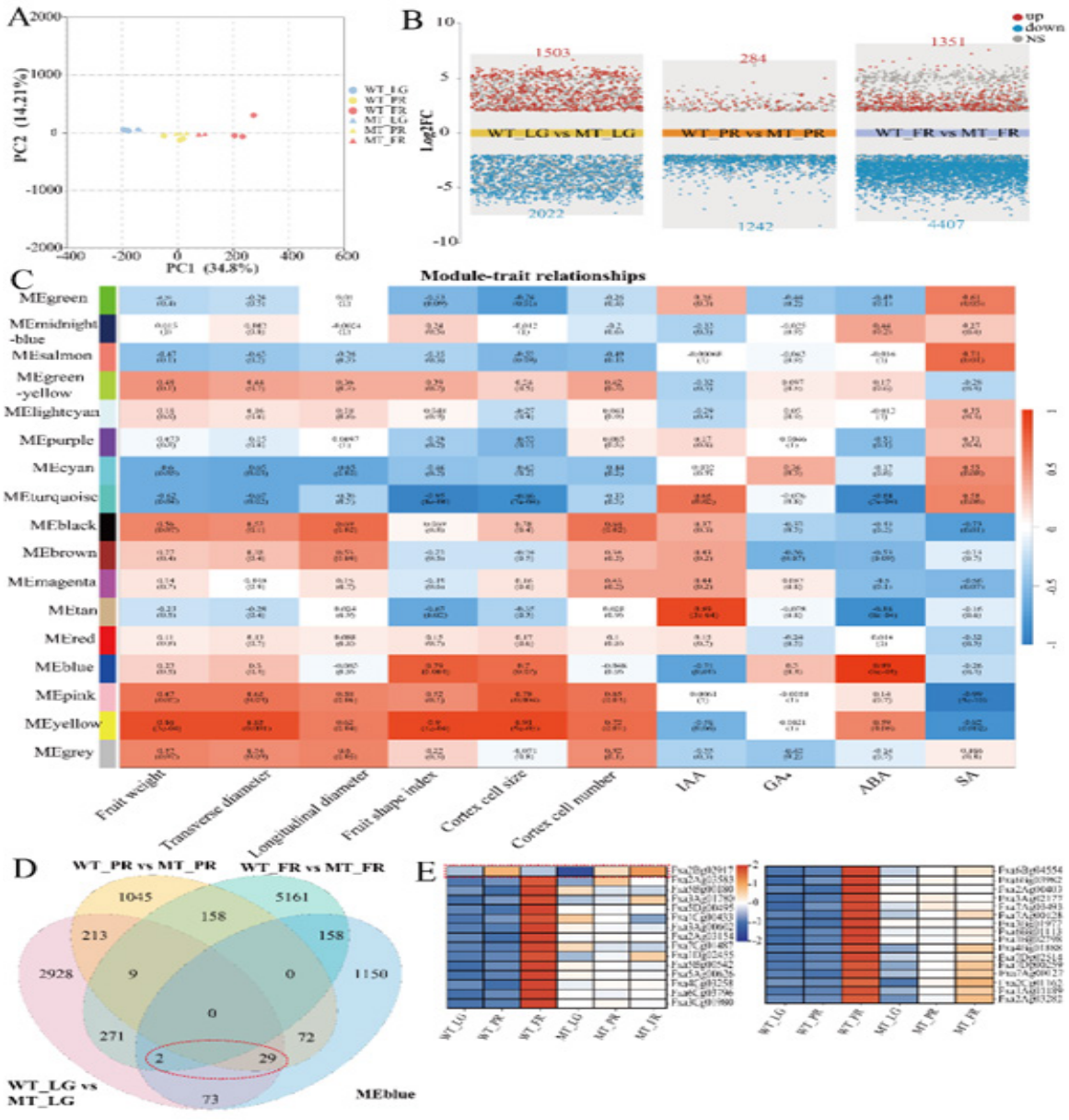

OPENPUB Global Publishers

Figure 5. Transcriptomic and co-expression network analysis during strawberry fruit development. PCA of transcriptomes in WT and MT fruits at LG, PR and FR stages (A), number of DEGs between WT and MT across three developmental stages (B), heatmap of module-trait correlations (C), intersection analysis of MEblue module genes and stage-specific DEGs, red dashed ellipse highlights overlapping genes (D), expression heatmap of overlapping genes, red dashed box marks candidate genes (E).

2.6 Transient-overexpression of FaIAA29 influences the growth of the cells and inhibits anthocyanin accumulation and ripening in strawberry fruit.

Phylogenetic tree analysis based on the Fxa2Bg02917 coding sequence showed that it clustered closely with woodland strawberry *FvIAA29*, leading to its designation as *FaIAA29* (Fig. 6A). The RT-qPCR results confirmed developmental expression patterns consistent with RNA-seq data (Fig. 6B). Spatiotemporal profiling demonstrated highest *FaIAA29* expression levels in roots, followed by stems, and minimal expression in flowers (Fig. 6C). Subcellular localization confirmed exclusive nuclear targeting (Fig. 6D).

Next, we conducted a transient overexpression (OE) experiment on the cultivated strawberry 'Benihoppe'. The study found that the relative expression level of *FaIAA29* in the transiently overexpressed fruits was 6.65 times that of the control (Fig. 6F), confirming the successful overexpression of *FaIAA29*. Observation of tissue structure at the injection site on the fruit surface showed that cell size at the *FaIAA29* OE site was significantly reduced compared to the control (Fig. 6G, H), while cell density was significantly increased (Figure 6I). Therefore, the primary function of *FaIAA29* is to negatively regulate cell size and positively regulate cell density.

In addition, we found that *FaIAA29* overexpression significantly inhibited strawberry fruits coloring (Fig. 6E), significantly reduced the *a** value (Fig. 6J), and significantly reduced the main anthocyanin components (Pg3G and cyanidin) in the fruits (Fig. 6K). Furthermore, we observed that anthocyanin synthesis genes were significantly downregulated (Fig. S2), indicating that *FaIAA29* negatively regulates strawberry fruit ripening and anthocyanin accumulation.

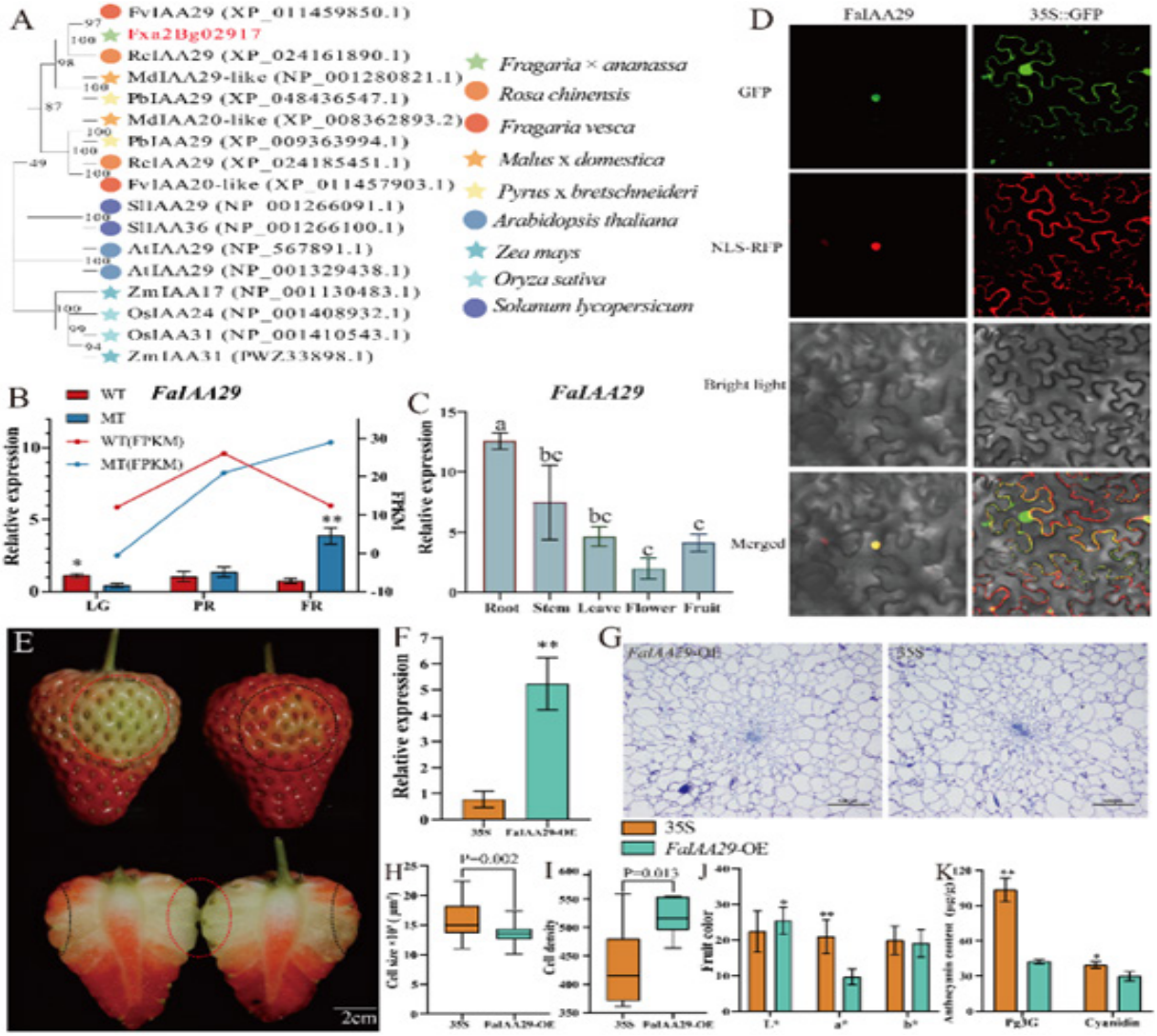

Figure 6. Functional characterization of *FaIAA29* in strawberry fruit development. Phylogenetic tree of IAA29 homologs (A), stage-specific expression of *FaIAA29* (B), tissue-specific expression of *FaIAA29* in root, stem, leaf, flower and fruit (C), subcellular localization of FaIAA29 protein (D), phenotypic comparison between *FaIAA29*-OE (red dashed ellipse) and empty vector control (black) (E), relative expression level of *FaIAA29* gene in control (35S) and *FaIAA29* -OE fruit (F), tissue structure (G), cell size (H), cell density (I), fruit color difference (J) and anthocyanin content (K).

2.7 The FaIAA29 associated co-expression network

Based on the MEblue module co-expression network, this study identified the top 20 genes most strongly correlated with *FaIAA29* (Fig. 7A, Table S5). The two genes exhibiting the highest correlation with *FaIAA29* were Fxa2Bg01459 and Fxa6Ag01022, annotated as Glutamate-tRNA Ligase (*FaGluRS*) and Mitochondrial Iron Transporter (*FaMIT*), respectively (Fig. S3A, B).

Potential binding sites for *FaIAA29* within the *FaGluRS* and *FaMIT* promoters were subsequently screened (Fig. 7B, C, S3C and Table S6). Y1H assays demonstrated that yeast cells harboring *FaIAA29* constructs bound to the P2 fragment of the *FaGluRS* promoter and the P1 and P3 fragments of the *FaMIT* promoter grew normally on selective medium (Fig. 7D, E). Dual-luciferase reporter assays revealed that *FaIAA29* strongly suppressed the transcriptional activity of the *FaGluRS* promoter but exhibited no significant regulatory effect on the *FaMIT* promoter (Fig. 7F, G). These results collectively validate the reliability of the co-expression network.

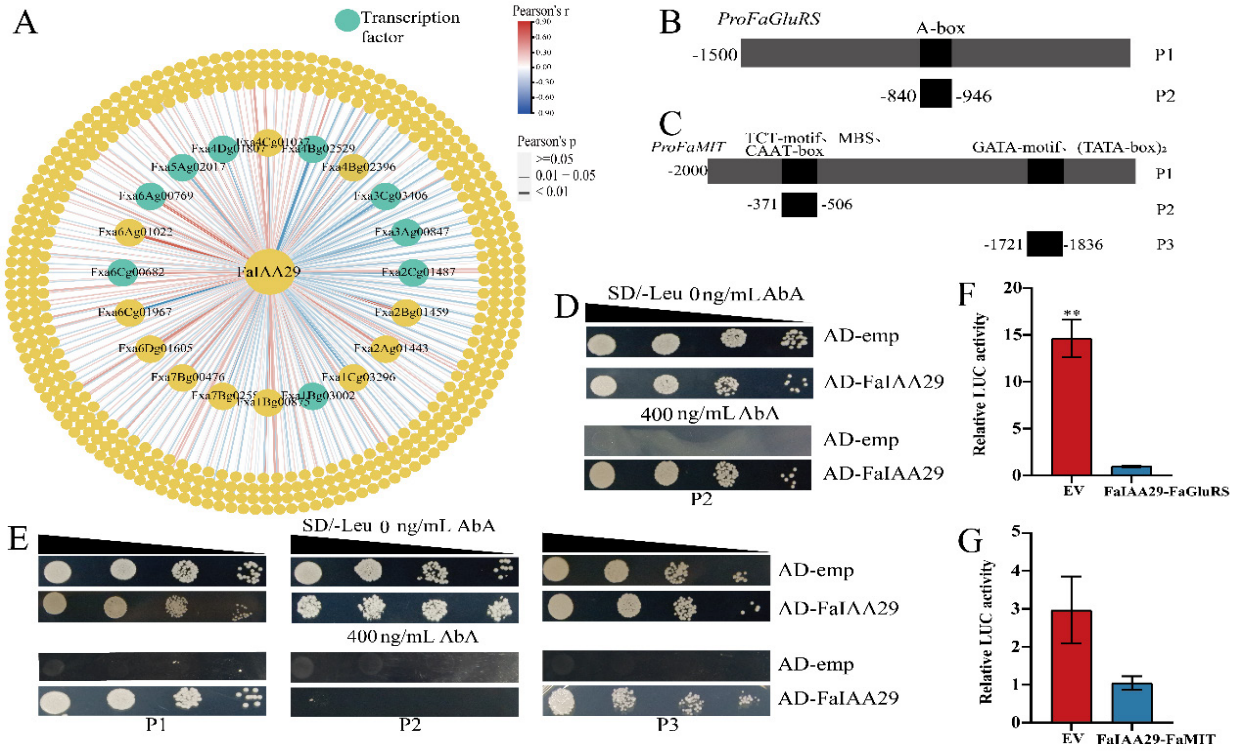

Figure 7. Co-expression network related to *FaIAA29*. *FaIAA29*-centric co-expression network in Meblue module (A), schematic representation of the *FaGluRS* (B) and *FaMIT* (C) promoters and their promoter fragments (P1-P3) cloned into pAbAi, Y1H validation of *FaIAA29* binding to *FaGluRS* (D) and *FaMIT* (E) promoter fragments, transcriptional repression of *FaGluRS* (F) and *FaMIT* (G) by *FaIAA29* as revealed by dual luciferase assay.

2.8 Transcriptome analysis of IAA and ABA signaling pathways in strawberry fruits

Correlation analyses explored molecular determinants underlying divergent IAA and ABA levels in WT and MT fruits. ABA level significantly associated with expression of *AUX/IAA*, *SAUR* and *PP2C* transcripts, while IAA level correlated with *AUX/IAA* and *SAUR* expression (Fig. 8A and Table S7). The above results indicate that differences in IAA and ABA levels may be closely related to their signaling pathways.

Heatmap analysis revealed that, in the IAA signaling pathway, *TIR1/AFB* expression levels decreased from LG to FR in WT, while remaining stable in MT. *AUX/IAAs* showed high expression in the LG and PR stages of WT, but expression levels decreased significantly in the FR stage. In MT, most *AUX/IAAs* also exhibited a decreasing trend in expression levels, though to a lesser extent. Notably, the expression levels of the two transcripts, Fxa2Bg02917 and Fxa2Dg02348, gradually increased in MT, which contrasts with the slow downregulation of other *AUX/IAA* expression levels during fruit development. *ARFs* expression levels were significantly higher in WT than in MT during the LG stage, but significantly lower during the FR stage. SAUR expression levels were significantly higher in WT than in MT during the LG phase. (Fig. 8B). In summary, the IAA signaling capacity in MT was weaker than in WT during the LG and PR stages, but it gradually increased from the PR to FR stages.

In the ABA signaling pathway, *PYR/PYL/RCAR*, *PP2C* and *SnRK2* are highly expressed during the LG and PR stages in WT. However, their expression levels are subsequently downregulated. In contrast, they remain low expression levels throughout fruit development in MT, with only the FR stage of MT showing higher expression than WT for these ABA signaling genes (Fig. 8C). We validated the expression patterns of some genes via RT-qPCR, which revealed trends consistent with those observed in the RNA-seq data (Fig. S5). In summary, the ABA signaling capacity in MT is weaker than in WT during the LG and PR stages, gradually increasing and then decreasing as the fruit matures.

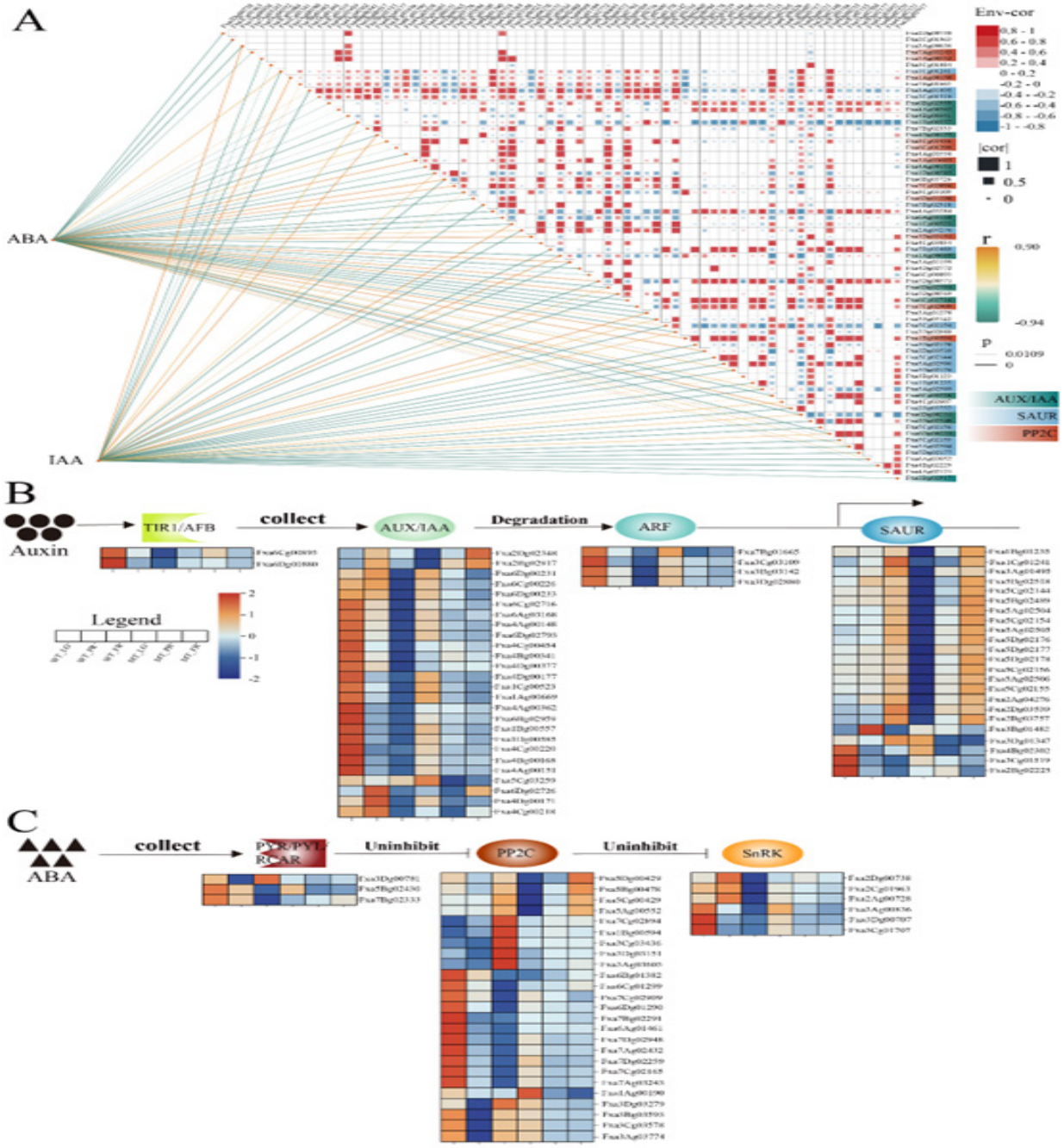

OPENPUB Global Publishers

Figure 8. Differences in IAA and ABA signaling and antagonism between the two underlie the differences in fruit size between WT and MT. correlation network of IAA and ABA (A), IAA (B) and ABA (C) signaling pathways.

3. Discussion

3.1 Strawberry fruit enlargement is accompanied by changes in quality traits

During the domestication of cultivated crops, the co-evolution of fruit morphology and quality is an important strategy for adapting to artificial selection pressures [21,22]. In strawberry [23] and sweet cherry [24], changes in fruit size are often accompanied by changes in flavor. In this study, a large-fruit mutant was identified during the cultivation of 'Benihoppe'. The size and weight of its ripe fruit were significantly greater than those of WT (Fig. 1A-D). However, its sugar and acid metabolism differed significantly from the WT. Sucrose content was significantly lower than WT throughout the MT's entire development process, while fructose and glucose content were significantly higher than WT starting from the PR stage (Figure 2A-C). Additionally, both fruit weight and transverse diameter were significantly and positively correlated with fructose and glucose content (Figure 4E). These findings are consistent with those of [23], who reported that large-fruited strawberry contain higher levels of fructose and glucose, as well as with the finding that the tomato tonoplast sugar transporter 3a (*TST3a*) mutant promotes fruit enlargement while increasing monosaccharide accumulation [25].

Anthocyanins are key compounds responsible for the color and health benefits of strawberry. Pg3G is the primary anthocyanin in mature strawberry fruit [26]. This study found that the Pg3G content of mature MT fruits was significantly lower than that of WT fruits (Figure 2H), which is consistent with the phenomenon of high anthocyanin accumulation in small strawberry fruits [23]. Notably, cyanidin accumulates continuously in MT fruits from the LG to FR stages. Both fruit weight and transverse diameter are significantly and positively correlated with cyanidin content (Fig. 2I and 4E). Together with reports that cyanidin is distributed in the epidermal layer of strawberries [27] and that there is a significant positive correlation between cortex cell size and cyanidin content, it is speculated that enlargement of MT cortex cells may increase cyanidin content.

3.2 Strawberry fruit size is primarily determined by the expansion of cortical cells

Strawberry fruit size is coordinately regulated by pith and cortical cells, with cellular expansion playing a pivotal role during development. While woodland strawberry relies primarily on pith cell enlargement for early fruit expansion, cortical cell expansion dominates post-veraison stages [28]. Our study reveal significant positive correlations between fruit weight and cortical cell size (Fig. 3E), indicating that accelerated cortical expansion is the primary driver of fruit enlargement in both WT and MT.

Among horticultural crops, fruit size is determined by the synergistic effects of cell number and volume, with regulatory strategies exhibiting species-specific divergence. Notably, apricot [14] and loquat [29] primarily utilize cell expansion for fruit enlargement, whereas sweet cherry [30] and apple [31] depend on combined cell division and expansion. This study found that the LG to PR stages represented the key developmental window for fruit size divergence between WT and MT (Fig. 3B-G). The enhanced cortical cell expansion in MT during LG to PR stages were the predominant factor underlying this divergence, while continued cell division in pith and cortex during veraison provided supplementary contribution to the oversized phenotype. This mechanism transcends the conventional limitation of fruit size determination by either cell number or size alone, thereby achieving the large-fruit phenotype in MT. Furthermore, our findings establish cellular size as a strategic breeding target for strawberry fruit size enhancement.

3.3 Auxin and ABA cooperatively regulate strawberry fruit development and ripening

Auxin and GA dominantly regulate strawberry fruit growth, whereas ABA governs ripening. Within the auxin signaling pathway, IAA induces TIR1/AFBs binding to Aux/IAA proteins, triggering their ubiquitin-mediated degradation and subsequent release of ARFs to activate downstream genes [11]. Transcriptomics revealed attenuated IAA signaling capacity in MT during LG and PR

stages but enhanced signaling at FR versus WT (Fig. 8B). *AUX/IAA* family members modulate fruit development or ripening across horticultural crops. For example, overexpression of *AUX/IAA* in watermelons increases flesh hardness and flesh cell number, while decreasing ABA content and flesh cell size [32]. Overexpression of *MdAux/IAA2* in apples inhibits fruit enlargement, weight and cell size [13]. Heterologous overexpression of *PpIAA1* in tomatoes promotes fruit ripening [33]. This study identified *FaIAA29* as a key gene that regulates strawberry fruit development and ripening. Transient overexpression of *FaIAA29* significantly reduced cell size and increased cell density (Fig. 6F-I) while inhibiting fruit coloration and anthocyanin accumulation (Fig. 6E, J and K). These results suggest that *FaIAA29* plays multiple roles, such as delaying coloration and promoting cell proliferation.

Although ABA plays an important role in regulating the ripening of non-climacteric fruits, there are currently no reports on the synergistic regulation of fruit development and ripening in horticultural crops by ABA and IAA. Strawberry fruit achenes accumulate IAA and ABA at specific sites of hormone interaction [34,16]. This study found that, during fruit development, the IAA level in MT was consistently higher than in WT, while the ABA level was consistently lower than in WT during the LG and FR stages (Fig. 4A, C). Additionally, the IAA and ABA levels exhibited a strong negative correlation (Fig. 4E), consistent with previously reported antagonism between the two. Additionally, MT's IAA and ABA signaling capabilities were weaker than WT's during the LG and PR stages, but stronger than WT's during the FR stage (Fig. 8C). The critical period for the size difference between MT and WT fruits was during the LG to PR stages. Therefore, the weakened IAA and ABA signaling capabilities of MT during the LG and PR stages may be closely related to differences in IAA and ABA accumulation, leading to enlargement of MT fruits.

4. Conclusion

Our study identified a stably inherited strawberry mutant of 'Benihoppe' whose fruit enlargement was primarily caused by intensified swelling of its cortex cells during the LG to PR period. However, continuous division of its pith and cortex cells during the PR to FR period also contributed to fruit enlargement. Additionally, as the fruit enlarges, the mutant shows higher accumulation of glucose, fructose, and IAA than 'Benihoppe,' while the Pg3G level is lower. ABA and IAA levels negatively correlate developmentally, and MT fruit enlargement is synergistically regulated by weakening IAA and ABA signaling during the LG to PR stages. Furthermore, we identified a key candidate gene, FaIAA29, that negatively regulates strawberry fruit cell size, color, and anthocyanin accumulation. Overexpression of *FaIAA29* promotes cell compaction and regulates the expression of the *FaGluRS* and *FaMIT* promoters. The results of this study provide new candidate gene resources for creating large-fruit strawberries and enrich our understanding of the synergistic regulation of strawberry fruit development and ripening by auxin-related genes.

Funding

This work was financially supported by the National Natural Science Foundation of China (No. 32272688); Key R&D Project of Science and Technology Department of Sichuan Province (No. 23ZDYF2968); Natural Science Foundation of Sichuan Province (No. 23NSFSC0777); Sichuan Tianfu New Area Rural Revitalization Research Institute "the open competition project to select the best candidates (Phase II projects)"; Tianfu New Area Chengdu-Deyang-Meishan-Ziyang Urban Modern Agricultural Park Fruits & Vegetables Expert-Doctoral Workstation Project.

Author contribution

Yilin Yang: Conceptualization, Date curation, Investigation, Writing - original draft, Writing - review & editing. **Zihang Ouyang**: Methodology, Investigation, Conceptualization. **Siqi Dai**: Methodology, Investigation. **Yuanxiu Lin**: Supervision. **Yunting Zhang**: Supervision. **Mengyao Li**: Methodology. **Qin Chen**: Methodology. **Yong Zhang**: Supervision. **Haoru Tang**: Funding acquisition, Resources. **Ya Luo**: Writing - review & editing, Funding acquisition, Conceptualization.

Data Availability

The data for MT strawberry fruits have been deposited in the NCBI SRA database under accession number PRJNA1261672. The expression profiles of WT strawberry fruits based on RNA-seq were retrieved from the NCBI SRA database (accession number: PRJNA838938). The data are presented within the paper and supplementary files.

Acknowledgements

The authors would express their appreciations to Zihang Ouyang for her help in experiments.

Conflict of interest statement

The authors declare no conflict of interest.

Supplementary data

Supplementary data is available in the supplementary files.

1. Zhao, X., Muhammad, N., Zhao, Z., Yin, K., Liu, Z., et al. (2021). Molecular regulation of fruit size in horticultural plants: A review. *Scientia Horticulturae*, *288*, 110353. https://doi.org/10.1016/j.scienta.2021.110353.

2. Sablowski, R., Carnier Dornelas, M. (2014). Interplay between cell growth and cell cycle in plants. *Journal of experimental botany*, *65*(10), 2703-2714. https://doi.org/10.1093/jxb/ert354.

3. Jorgensen, P., Tyers, M. (2004). How cells coordinate growth and division. *Current biology*, *14*(23), R1014-R1027. https://doi.org/10.1016/j.cub.2004.11.027.

4. Cong, B., Liu, J., Tanksley, S. D. (2002). Natural alleles at a tomato fruit size quantitative trait locus differ by heterochronic regulatory mutations. *Proceedings of the National Academy of Sciences*, *99*(21), 13606-13611. https://doi.org/10.1073/pnas.172520999.

5. Li, Q., Chakrabarti, M., Taitano, N. K., Okazaki, Y., Saito, K., et al. (2021). Differential expression of SlKLUH controlling fruit and seed weight is associated with changes in lipid metabolism and photosynthesis-related genes. *Journal of experimental botany*, *72*(4), 1225-1244. https://doi.org/10.1093/jxb/eraa518.

6. Gal, T. Z., Aussenberg, E. R., Burdman, S., Kapulnik, Y., Koltai, H. (2006). Expression of a plant expansin is involved in the establishment of root knot nematode parasitism in tomato. Planta. 224, 155-162. https://doi.org/10.1007/s00425-005-0204-x.

7. Kuluev, B.R., Kniazev, A.V., Nikonorov, I.M., Chemeris, A.V. (2014). Role of the expansin genes *NtEXPA1* and *NtEXPA4* in the regulation of cell extension during tobacco leaf growth. Genetika. 50, 560-569. (Russian).

8. Choi, D., Lee, Y., Cho, H.T., Kende, H. (2003). Regulation of Expansin Gene Expression Affects Growth and Development in Transgenic Rice Plants. Plant Cell 15, 1386–1398. https://doi.org/10.1105/tpc.011965.

9. Ozga, J. A., Reinecke, D. M. (2003). Hormonal Interactions in Fruit Development. J. Plant Growth Regul. 22, 73-81. https://doi.org/10.1007/s00344-003-0024-9.

10. Dharmasiri, N., Estelle, M. (2004). Auxin signaling and regulated protein degradation. Trends Plant Sci. 9, 302-308. https://doi.org/10.1016/j.tplants.2004.04.003.

11. Rademacher, E. H., Möller, B., Lokerse, A. S., Llavata-Peris, C. I., van den Berg, W., Weijers, D. (2011). A cellular expression map of the *Arabidopsis AUXIN RESPONSE FACTOR* gene family. Plant J. 68, 597-606. https://doi.org/10.1111/j.1365-313X.2011.04710.x.

12. Su, L., Bassa, C., Audran, C., Mila, I., Cheniclet, C., Chevalier, C., et al. (2014). The auxin *Sl-IAA17* transcriptional repressor controls fruit size via the regulation of endoreduplication-related cell expansion. Plant Cell Physiol. 55, 1969-1976. https://doi.org/10.1093/pcp/pcu124.

13. Bu, H., Sun, X., Yue, P., Qiao, J., Sun, J., et al. (2022). The *MdAux/IAA2* Transcription Repressor Regulates Cell and Fruit Size in Apple Fruit. Int. J. Mol. Sci. 23, 9454. https://doi.org/10.3390/ijms23169454.

14. Huang, M., Zhu, X., Bai, H., Wang, C., Gou, N., et al. (2023). Comparative anatomical and transcriptomics reveal the larger cell size as a major contributor to larger fruit size in Apricot. Int. J. Mol. Sci. 24, 8748. https://doi.org/10.3390/ijms24108748.

15. Jia, H. F., Chai, Y. M., Li, C. L., Lu, D., Luo, J. J., et al. (2011). Abscisic acid plays an important role in the regulation of strawberry fruit ripening. Plant Physiol. 157, 188-199. https://doi.org/10.1104/pp.111.177311.

16. Liao, X., Li, M., Liu, B., Yan, M., Yu, X., et al. (2018). Interlinked regulatory loops of ABA catabolism and biosynthesis coordinate fruit growth and ripening in woodland strawberry. Proc. Natl. Acad. Sci. U.S.A. 115, E11542-E11550. https://doi.org/10.1073/pnas.1812575115.

17. Li, B. J., Shi, Y. N., Xiao, Y. N., Jia, H. R., Yang, X. F., et al. (2024). AUXIN RESPONSE FACTOR 2 mediates repression of strawberry receptacle ripening via auxin-ABA interplay. Plant Physiol. 196, 2638-2653. https://doi.org/10.1093/plphys/kiae510.

18. Li, Q., Wang, J., Yin, Z., Pan, Y., Mao, W., et al. (2024). SlPP2C2 interacts with FZY/SAUR and regulates tomato development via signaling crosstalk of ABA and auxin. Plant J. 119, 1073–1090. https://doi.org/10.1111/tpj.16818.

19. Kang, C., Darwish, O., Geretz, A., Shahan, R., Alkharouf, N., Liu, Z. (2013). Genome-scale transcriptomic insights into early-stage fruit development in woodland strawberry *Fragaria vesca*. Plant Cell. 25, 1960-1978. https://doi.org/10.1105/tpc.113.111732.

20. Chen, Q., Yu, H. W., Wang, X. R., Xie, X. L., Yue, X. Y., Tang, H. R. (2012). An alternative cetyltrimethylammonium bromide-based protocol for RNA isolation from blackberry (*Rubus l.*). Genet. Mol. Res. 11, 1773–1782. https://doi.org/10.4238/2012.June.29.10.

21. Du, Q., Yu, H., Zhang, Y., Qiao, Q., Wang, J., Zhang, T., Xue, L., Lei, J., (2024). Uncovering fruit flavor and genetic diversity across diploid wild *Fragaria* species via comparative metabolomics profiling. Food Chem. 456, 140013. https://doi.org/10.1016/j.foodchem.2024.140013.

22. Ma, B., Chen, J., Zheng, H., Fang, T., Ogutu, C., et al. (2015). Comparative assessment of sugar and malic acid composition in cultivated and wild apples. Food Chem. 172, 86-91. https://doi.org/10.1016/j.foodchem.2014.09.032.

23. Simkova, K., Veberic, R., Hudina, M., Grohar, M.C., Ivancic, T., et al. (2023). Berry size and weight as factors influencing the chemical composition of strawberry fruit. J. Food Compos. Anal. 123, 105509. https://doi.org/10.1016/j.jfca.2023.105509.

24. Aglar, E., Saracoglu, O., Ozturk, B., Karakaya, O., Ateş, U., 2023. The Influence of Fruit Size on Quality Attributes and Bioactive Compounds of Sweet Cherry Fruit. Erwerbs-Obstbau. 65, 701–707. https://doi.org/10.1007/s10341-022-00726-2.

25. Cai, H., Liang, M., Qin, X., Dong, R., Wang, X., et al. (2025). Tonoplast sugar transporters coordinately regulate tomato fruit development and quality. Plant Commun. 6, 101314. https://doi.org/10.1016/j.xplc.2025.101314.

26. Afrin, S., Gasparrini, M., Forbes-Hernandez, T.Y., Reboredo-Rodriguez, P., Mezzetti, B., et al. (2016). Promising Health Benefits of the Strawberry: A Focus on Clinical Studies. J. Agric. Food Chem. 64, 4435-4449. https://doi.org/10.1021/acs.jafc.6b00857.

27. Enomoto, H., Sato, K., Miyamoto, K., Ohtsuka, A., Yamane, H (2018). Distribution analysis of anthocyanins, sugars, and organic acids in strawberry fruits using matrix-assisted laser desorption/ionization-imaging mass spectrometry. J. Agric. Food Chem. 66, 4958-4965. https://doi.org/10.1021/acs.jafc.8b00853.

28. Li, Y., Zhang, P., Wang, G., Zhao, W., Bao, Z., Ma, F., (2024). *FvUVI4* inhibits cell division and cell

expansion to modulate fruit development in *Fragaria vesca*. Plant Physiol. Biochem. 213, 108804. https://doi.org/10.1016/j.plaphy.2024.108804.

29. Su, W., Shao, Z., Wang, M., Gan, X., Yang, X., Lin, S (2021). EjBZR1 represses fruit enlargement by binding to the *EjCYP90* promoter in loquat. Hortic. Res. 8, 152. https://doi.org/10.1038/s41438-021-00586-z.

30. Olmstead, J.W., Iezzoni, A.F., Whiting, M.D., (2007). Genotypic Differences in Sweet Cherry Fruit Size are Primarily a Function of Cell Number. J. Am. Soc. Hortic. Sci. 132, 697-703. https://doi.org/10.21273/JASHS.132.5.697.

31. Harada, T., Kurahashi, W., Yanai, M., Wakasa, Y., Satoh, T. (2005). Involvement of cell proliferation and cell enlargement in increasing the fruit size of *Malus* species. Sci. Hortic. 105, 447-456. https://doi.org/10.1016/j.scienta.2005.02.006.

32. Anees, M., Zhu, H., Umer, M.J., Gong, C., Yuan, P., et al. (2024). Identification of an Aux/IAA regulator for flesh firmness using combined GWAS and bulked segregant RNA-Seq analysis in watermelon. Hortic. Plant J. 10, 1198-1213. https://doi.org/10.1016/j.hpj.2023.05.018.

33. Wang, X., Pan, L., Wang, Y., Meng, J., Deng, L., et al. (2021). *PpIAA1* and *PpERF4* form a positive feedback loop to regulate peach fruit ripening by integrating auxin and ethylene signals. Plant Sci. 313, 111084. https://doi.org/10.1016/j.plantsci.2021.111084.

34. Li, T., Dai, Z., Zeng, B., Li, J., Ouyang, J., Kang, L., et al. (2022). Autocatalytic biosynthesis of abscisic acid and its synergistic action with auxin to regulate strawberry fruit ripening. Hortic Res. 9, uhab076. https://doi.org/10.1093/hr/uhab076.

35. Jiang, L., Yue, M., Liu, Y., Zhang, N., Lin, Y., et al. (2023). A novel R2R3-MYB transcription factor FaMYB5 positively regulates anthocyanin and proanthocyanidin biosynthesis in cultivated strawberries (*Fragaria* × *ananassa*). Plant Biotechnol J. 21, 1140–1158. https://doi.org/10.1111/pbi.14024.